Visualizing Nano-Electromechanics by Vector Piezoresponse Force Microscopy

B.J. Rodriguez,[1] S. Jesse,[2] A.P. Baddorf,[2] S.V. Kalinin,[2] A. Gruverman[1]

[1]Department of Materials Science and Engineering, North Carolina State University, Raleigh, NC 27695
[2]Condensed Matter Sciences Division, Oak Ridge National Laboratory, Oak Ridge, TN 37831

ABSTRACT

A novel approach for nanoscale imaging and presentation of the orientation dependence of electromechanical properties, vector piezoresponse force microscopy (Vector-PFM), is proposed. The relationship between local polarization, piezoelectric constants and crystallographic orientation is described. The image formation mechanism in vector PFM and conditions for complete three-dimensional (3D) reconstruction of the electromechanical response vector and evaluation of the piezoelectric constants from PFM data are discussed. The developed approach can be applied to crystallographic orientation imaging in piezoelectric materials with a spatial resolution below 10 nm. Several approaches for data representation in two-dimensional (2D)-PFM and 3D-PFM are described.

Keywords: scanning probe microscopy, piezo response force microscopy, vector PFM,

1 INTRODUCTION

In the last decade, Piezoresponse Force Microscopy (PFM) has been established as a primary technique for imaging and non-destructive characterization of piezoelectric and ferroelectric materials on the nanometer scale.[1,2,3,4] The term piezoresponse, introduced in Ref. [4] for the description of this voltage-modulated contact mode of scanning probe microscopy, comes from the fact that the measured signal is dominated by the piezoelectric deformation of the ferroelectric sample. In the original papers on PFM, only the normal component of the tip displacement related to the out-of-plane component of polarization vector has been measured, an approach further referred to as vertical PFM (VPFM).[5] In 1998, Eng et al.[6,7] proposed a lateral PFM (LPFM) imaging method for measuring the in-plane component of polarization by monitoring the angular torsion of the cantilever. However, it is recognized that the electromechanical response is a vector having three independent components, while vertical and lateral PFM provide only two independent components. To address this problem, an approach for three-dimensional (3D) reconstruction of polarization using a combination of the VPFM data with two LPFM data sets obtained at different scanning directions has been developed.[6,8] However, in these experiments the absolute sensitivities in vertical and lateral directions were not calibrated, precluding the unambiguous reconstruction of the piezoresponse vector. The analysis by Kalinin et al.[9] has shown that the measured PFM signal also depends on local elastic properties, necessitating simultaneous measurement of the latter. Here, we discuss the information on local materials properties that can be obtained from quantitative measurements of full electromechanical response vector, an approach further referred to as Vector PFM, principles of the technique and its resolution limits. Vector PFM is shown to be a powerful tool for local orientation imaging in piezoelectrically active materials, such as micro- and nanocrystalline ferroelectric thin films and biological systems.

2 PRINCIPLES OF PFM

Piezoresponse force microscopy is based on the detection of the bias-induced piezoelectric surface deformation. The tip is brought into contact with the surface, and the piezoelectric response of the surface is detected as the first harmonic component, $A_{1\omega}$, of the tip deflection, $A = A_0 + A_{1\omega}\cos(\omega t + \varphi)$, induced by the application of the periodic bias $V_{\text{tip}} = V_{\text{dc}} + V_{ac}\cos(\omega t)$ to the tip. Here, the deflection amplitude, $A_{1\omega}$, is assumed to be calibrated and given in the units of length. When applied to the pyroelectric or ferroelectric materials, the phase of the electromechanical response of the surface, φ, yields information on the polarization direction below the tip.

Application of the bias to the tip results in the surface displacement, **w**, with both normal and in-plane components, $\mathbf{w} = (w_1, w_2, w_3)$. The usual assumption in the interpretation of PFM data is that the displacement of the tip apex in contact with the surface is equal to the surface displacement.[10] This is reasonable since the effective spring constant of the tip-surface junction is typically 2-3 orders of magnitude higher than the cantilever spring constant.

In addition to the vertical component of tip deflection, the use of a four-quadrant photodetector allows the lateral piezoresponse component in the direction normal to the cantilever axis (lateral transversal displacement) to be determined as torque of the cantilever. The fundamental difference between VPFM and LPFM is that in the latter case the displacement of the tip apex can be significantly smaller than that of the surface, e.g. due to the onset of sliding friction. Therefore, while in VPFM the response amplitude is expected to scale linearly with the modulation amplitude, in LPFM the response amplitude will eventually saturate. This sliding friction also minimizes the contribution from the piezoresponse component along the

cantilever axis (lateral longitudinal displacement), as discussed in detail elsewhere.[11]

Information on the response component along the cantilever is usually difficult to obtain and in most cases only a 2D image can be acquired. For 3D imaging the second lateral component has to be measured by physically rotating the sample with respect to the cantilever as a simple change of the scan angle will not produce this result. This requirement necessitates locating the same microscale region on the surface after sample rotation, a task which is possible only for the samples with clear microscopic topographic markers.

The next step in the interpretation of the PFM data is detailed analysis of materials properties that can be extracted from the displacement vector. Assuming the scanning probe microscope is properly calibrated, the set of the piezoresponse data can be converted into the full electromechanical response vector, $\mathbf{w} = (w_1, w_2, w_3)$. The piezoelectric properties of materials are described by the third-order piezoelectric constant tensor d_{ij}, where i = 1,..,3, j = 1, .., 6, that defines the relationship between the strain tensor and the electric field: $X_j = d_{ij} E_i$.[12] Here, the components of d_{ij} are given in the laboratory coordinate system, in which axis 3 is normal to the surface and axis 1 is oriented along the long cantilever axis and the reduced Voigt notation[13] is used. The piezoresponse signal measured in the PFM experiment has the same dimensionality as the piezoelectric constants, suggesting the close relationship between d_{ij} and components of the electromechanical surface response vector. This is remarkable, since PFM is thus an SPM technique, which is sensitive to the tensorial properties of materials. In the local excitation case, the PFM signal can be semi-quantitatively approximated as $vPR_l = d_{33}$, $xPR_l = d_{35}$ and $yPR_l = d_{34}$, where the coordinate system for d_{ij} is laboratory coordinate system related to the cantilever orientation. For materials with known crystallographic orientation, the elements of the d_{ij}^0 tensor can be semiquantitatively determined by VPFM, 2D- or 3D-PFM measurements performed on crystals with different orientations. For materials with known piezoelectric constants, d_{ij}^0, the local crystallographic orientation in each point (orientation imaging) can be determined from vector 3D-PFM data. For materials systems with known constraints on possible crystallographic orientation (small number of domains), domain structure reconstruction can be obtained from partial VPFM or 2D-PFM data.

3 MODELLING SIGNAL GENERATION

One of the outstanding questions in PFM and mechanical modulation techniques such as Atomic Force Acoustic Microscopy is the signal generation volume that determines both lateral resolution and depth sensitivity. Both of these techniques are ultimately sensitive to bias and displacement-induced changes in indentation depth. The complete description of the nanoelectromechanics of piezoelectric indentation for a special case of transversally isotropic material as applied to PFM and AFAM was given by Kalinin and Karapetian.[9,10]

In particular, from the known displacement field below the tip, the signal generation volume in PFM can be found as $\delta u_z / \delta V$, whereas in AFAM the signal generation volume is $\delta u_z / \delta d$, where $u_z = u_z(\rho, z)$ is the normal displacement field below the tip and δu_z is its change in response to the change in tip potential, δV, or sample base position, δd. For piezoelectric indentation, the normal displacement field could be represented as a linear superposition of the fields $u_z = u_{z,m}(a) + u_{z,e}^0(a)\psi_0$. Here $u_{z,m}$ is the solution of the indentation problem with purely mechanical boundary conditions and zero potential and $u_{z,e}^0(a,R)\psi_0$ is the solution of the purely electrical problem. Shown in Figure 1a,b is the vector map of electrical field inside material induced by tip bias for a = 5 nm and R = 50 nm for PZT6b and $BaTiO_3$ respectively. The field distribution and penetration depth is determined primarily by anisotropy of the dielectric constant tensor of the material. Figure 1c,d illustrate the strain field induced by the mechanical load applied to the tip. In both cases, the electromechanical coupling affects the corresponding field distributions only weakly, as can be shown by comparison with similar maps calculated for zero electromechanical coupling, $e_{ij} = 0$. Finally, shown in

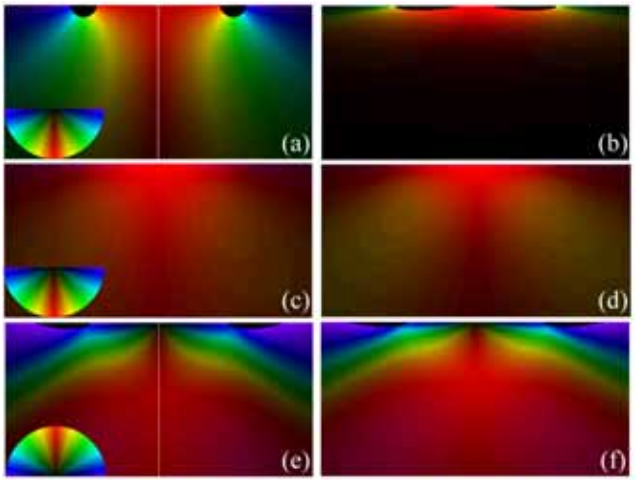

Figure 1:Vector map of electric field magnitude and direction induced by tip bias for PZT6b (a) and $BaTiO_3$ (b). Brightness indicates the magnitude of electric field, whereas color indicates direction. Shown is map for ($\ln(E_\rho)$,$\ln(E_z)$), where E_ρ and E_z is lateral and vertical components of electric field. Vector maps for indentation-force induced strain field below the tip for PZT6b (c) and $BaTiO_3$ (d). Shown is map for (u_ρ,u_z), where u_ρ and u_z are lateral and vertical strain components. Vector map for bias induced strain field below the tip for PZT6b (e) and $BaTiO_3$ (f). Shown is map for (u_ρ,u_z), where u_ρ and u_z are lateral and vertical strain components.

Figure 1e,f is the strain field induced by the bias applied to the tip, which originates directly from electromechanical coupling.

This analysis suggests that the signal generation volume, and hence resolution, is limited by the contact area between the tip and the surface, typically of order of 3-5 nanometers. This is in a close agreement with experimentally observed resolution in PFM of order of 5-10 nm, suggesting the potential of Vector PFM to image local electromechanical properties with sub-10nm resolution.

4 EXPERIMENTAL RESULTS

An outstanding issue for the Vector PFM is image representation. While for most SPMs the use of pseudocolor images is common, the color is generally used for the enhancement of the contrast of the scalar data. Here we demonstrate two approaches to represent 2D and 3D Vector PFM data. Shown in Figure 2a,b are vertical and lateral PFM, $A_{1\omega}\cos(\varphi)$ signals, from $PbTiO_3$ thin film. In the VPFM image, high intensity corresponds to the regions with a strong vertical component of electromechanical response in a positive *z*-direction, while low intensity corresponds to a strong response in the negative *z*-direction. Gray areas of intermediate intensity correspond to a weak out-of-plane response component. Similarly, the LPFM image provides information on the in-plane component perpendicular to the cantilever axis. Upon close examination, the PFM images in Figure 2a,b show a decrease of the effective PFM signal in the center of the grain. Such behavior can be attributed to a change in magnitude of the electro-mechanical response vector, either due to an intrinsic change of the material's properties or tip-surface contact. However, interpretation of separate LPFM and VPFM data is not straightforward.

To address this problem, we employ vector representation for PFM data similar to an approach well-known in electron microscopy. The VPFM and LPFM images are normalized with respect to the maximum and minimum values of the signal amplitude so that the intensity changes between -1 and 1, i.e. $vpr, lpr \in (-1,1)$. While not strictly rigorous, this procedure is expected to provide the correct answer for systems where grains with all possible orientations of the response vector are present. Using commercial software,[14] these 2D vector data (vpr, lpr) are converted to the amplitude/angle pair, $A_{2D} = \mathrm{Abs}(vpr + I\ lpr)$, $\theta_{2D} = \mathrm{Arg}(vpr + I\ lpr)$. These data then used to generate a pseudocolor map where the color corresponds to the orientation, while color intensity corresponds to the magnitude of the response vector, as illustrated in Figure 2c. We refer to this method for PFM data representation as a 2D vector PFM image. Here both color and intensity convey information and the "color wheel" legend illustrates the direction and magnitude of the response vector.

Notably, the vector-PFM image illustrates that color is virtually uniform inside the grains, while the intensity varies between the central part of the grain and the circumference. This difference illustrates that only the magnitude, but not the orientation, of the piezoresponse vector changes. This information can be represented in the scalar form by plotting separately phase, θ_{2D}, and magnitude, A_{2D}, data, as illustrated in Figure 2d,e, respectively. In the phase image (Figure 2d), the phase of the 2D response vector is clearly uniform within individual grains, whereas magnitude (Figure 2e) changes from the grain center to its circumference.

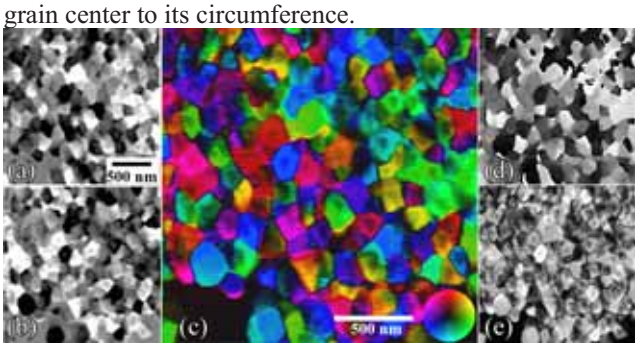

Figure 2: Vertical (a) and lateral (b) PFM image of PZT thin film. (c) Vector representation of 2D PFM data. (d) Angle and (e) amplitude images.

An example of 3D-PFM imaging is illustrated in Figure 3 using an etched $LaBGeO_5$ glass ceramic. Figure 3a is an image showing the 3D vector piezoresponse of the ferroelectric grain. Because of the relatively large grain size (~50 μm), the same region could be imaged several times with different orientations of the cantilever relative to the sample, thus allowing 3D PFM data to be collected. Here, VPFM, *x*-LPFM and *y*-LPFM data sets containing information on all three components of the electro-mechanical response vector were collected.

The representation of complete 3D vector field, as opposed to a 2D subset, represents a more challenging problem. The solution requires using the entire color palette available including hue, intensity, and lightness. Here, the VPFM and *x*,*y* LPFM images are normalized with respect to the maximum and minimum values of the signal amplitude so that the intensity changes between -1 and 1, i.e. $vpr, xlpr, ylpr \in (-1,1)$. These 3D vector data $(vpr, xlpr, ylpr)$ are mapped on the red, green, blue color scale, represented as vector (R, G, B), where *R*, *G* and *B* are mutually orthogonal and vary from 0 to 1. The magnitude of the *z*-component is represented by lightness/darkness, variation in direction in the *x*,*y*-plane is given by hue, and the magnitude of the vector is represent by color saturation (note that black and white are colors).

The transformation involves rotating the (R, G, B) coordinate system and shifting it so that $(R, G, B) = (0.5,\ 0.5,\ 0.5)$ corresponds to zero in the PFM coordinate system, $(vpr, xlpr, ylpr) = (0,0,0)$. This transformation is expressed in the equations:

$$(R \quad G \quad B) = \frac{1}{2}\left[\frac{1}{\sqrt{3}}\cdot\left(R_x(\theta)\cdot R_z(\phi)\right)^T\cdot(xlpr \quad ylpr \quad vpr) + (1 \quad 1 \quad 1)\right]$$

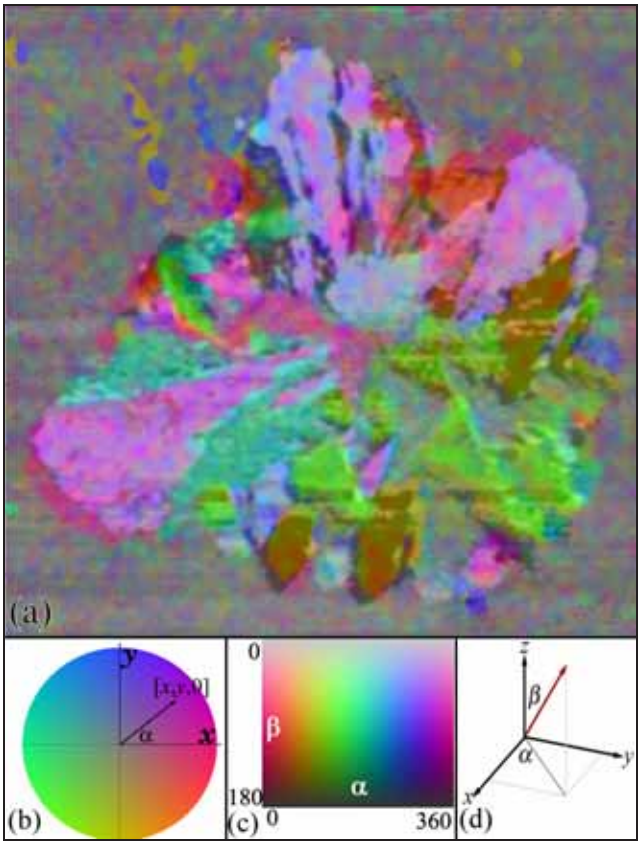

Figure 3: (a) 3D vector piezoresponse representation of an etched $LaBGeO_5$ glass ceramic. (b) color wheel map relating hue to lateral piezoresponse. (c) map relating vector direction to color for a unit vector. (d) relationship between angles in (c) and laboratory coordinate system.

where $R_x(\theta_r)$ and $R_z(\phi_r)$ are rotation matrices and $\theta_r = \tan^{-1}\sqrt{2}$ and $\phi_r = \pi/4$ are Euler angles.

Note that light shading indicates the vector pointing out of the page and dark shading indicates a vector pointing into the page. This relationship is shown in the color key in Figure 3c in accordance with the coordinate axis in Figure 3d. Gray areas indicate regions where the magnitude of the response vector is relatively small. Intense or saturated hues indicate a strong lateral response with small a vertical component. This is represented in the color wheel in Figure 3b which shows the color coding for purely lateral displacement vectors (no vertical component).

5 CONCLUSIONS

An approach for vector electromechanical imaging by SPM, referred to as vector piezoresponse force microscopy (Vector PFM), is proposed. The relationship between detected vertical and lateral signal components and local electromechanical response vector is discussed. The relationship between 3D-PFM data and local materials' properties is established and it is shown that 3D PFM can be used as a powerful tool for (a) local electromechanical property measurements on the nanoscale or (b) local orientation imaging on the sub-10 nm level. Finally, several approaches for data representation in 2D-PFM and 3D-PFM are presented. The developed approach can be applied for nanoscale electromechanical characterization of a broad range of material systems including polymers, composites, and biomaterials.

ACKNOWLEDGEMENTS

Research performed in part as a Eugene P. Wigner Fellow and staff member at the Oak Ridge National Laboratory, managed by UT-Battelle, LLC, for the U.S. Department of Energy under Contract DE-AC05-00OR22725 (SVK). Support from ORNL SEED funding is acknowledged (ABP and SVK). AG acknowledges financial support of the National Science Foundation (Grant No. DMR02-35632). $LaBGeO_5$ sample is courtesy of P. Gupta, H. Jain, and D.B. Williams (Lehigh).

[1] *Ferroelectrics at Nanoscale: Scanning Probe Microscopy Approach*, edited by M. Alexe and A. Gruverman (Springer Verlag, 2004).

[2] *NanoScale Phenomena in Ferroelectric Thin Films,* edited by S. Hong (Kluwer Academic Publishers, Boston, 2004).

[3] P. Gunther and K. Dransfeld, Appl. Phys. Lett. **61**, 1137 (1992).

[4] A.Gruverman, O.Auciello and H.Tokumoto, J. Vac. Sci. Technol. **B 14**, 602-605 (1996).

[5] A. Gruverman, O. Auciello, and H. Tokumoto, Annu. Rev. Mat. Sci. **28**, 101-123 (1998).

[6] L.M. Eng, H.-J. Guntherodt, G.A. Schneider, U. Kopke and J.M. Saldana, Appl. Phys. Lett. **74**, 233 (1999)

[7] L. M. Eng, H.-J. Güntherodt, G. Rosenman, A. Skliar, M. Oron, M. Katz, and D. Eger, , J. Appl. Phys. **83**, 5973-5977 (1998).

[8] B.J. Rodriguez, A. Gruverman, A.I. Kingon, R.J. Nemanich, and J.S. Cross, J. Appl. Phys. **95**, 1958 (2004).

[9] Sergei V. Kalinin, E. Karapetian, and M. Kachanov, Phys. Rev. B 70, 184101 (2004)

[10] E. Karapetian, M. Kachanov, and S.V. Kalinin, , Phil. Mag., in print

[11] Sergei V. Kalinin, B.J. Rodriguez, S. Jesse, J. Shin, A.P. Baddorf, P. Gupta, H. Jain, D.B. Williams, and A. Gruverman, Microscopy and Microanalysis, submitted

[12] *Physical Properties of Crystals,* J.F. Nye, (Oxford University Press, 1985).

[13] Due to symmetry, the indices i,j in full piezoelectric coefficient tensor, d_{ijk}, and strain tensor, X_{ij}, are substituted as 11→1, 22→2, 33→3, 12→ 6, 13→ 5, 23→ 4.

[14] Mathematika 5.0, Wolfram Research